

AN INTEGRO-DIFFERENTIAL MODEL FOR THE DYNAMICS OF AEOLIAN SAND RIPPLES

HEZI YIZHAQ,¹ NEIL J. BALMFORTH,² ANTONELLO PROVENZALE^{1,3}

¹*I.S.I Foundation, V.le. Settimio Severo 65, I-10133 Torino, Italy. E-mail address: hezi@andromeda.isi.it,* ²*Dept. of Applied Mathematics and Statistics, UCSC, Santa Cruz, CA 95064, USA. E-mail address: njb@cse.ucsc.edu,* ³*CNR-ISAC, Corso Fiume 4, I-10333 Torino, Italy. E-mail address: a.provenzale@isac.cnr.it*

Abstract

We discuss an integro-differential model for the nonlinear dynamics of aeolian sand ripples. The model is based on the classic approach of Anderson (1987) and includes a correction to the reptation flux that depends on the local bed slope. Linear stability analysis shows that a flat bed is unstable to perturbations in a narrow range of wavenumbers. As the ripple amplitude grows, nonlinear effects become important, ripples become asymmetric and their wavelength increases due to merging events.

1. Introduction

Aeolian ripples are commonly found in sand deserts, often atop dunes and on sandy beaches. Ripple wavelengths range from a few centimeters to tens of meters, and ripple amplitudes range from a few millimeters to a maximum of a few centimeters (Sharp, 1963; Wilson, 1972). A classic reference to ripples and dunes is the book “The Physics of Blown Sand and Desert Dunes” by R.A. Bagnold (1941). A theoretical model for the dynamics of aeolian ripples has been proposed by Anderson (1987), and it is used here as a starting point for our own formulation. Recently, there has been a resurgence of interest in developing mathematical models of the dynamics of aeolian ripples, a fact that has led to a series of papers based on different types of phenomenological and mathematical assumptions (Nishimori and Ouchi, 1993; Werner and Gillespie, 1993; Hoyle and Woods, 1997; Terzidis et al., 1998; Prigozhin, 1999; Valance and Rioual, 1999; Cshaók et al, 2000; Makse, 2000; Balmforth et al., 2001)

The physical mechanism responsible for the formation of sand ripples is thought to be the action of the wind on loose sand. When the wind strength is above some threshold, grains are displaced by the direct action of the wind, and are lifted into the air. Even for strong winds, however, sand grains are too heavy to stay suspended and return to the ground. During their flight, the grains reach a velocity that is approximately that of the wind, and upon their impact with the surface, they impart their energy and momentum to the sand, and eject other grains. For sufficiently large wind velocities, the bombardment by sand grains accelerated by the wind generates a cascade process, and an entire population of saltating grains hopping on the sand surface emerges. During strong winds, the layer of saltating grains can reach a thickness of more than one meter.

Experimental results (Anderson, 1987) indicate that the bombardment process generates two populations of moving grains: grains that are ejected with large energy

form one component of the population; these grains reach higher elevations and are directly accelerated by the wind. The high-energy grains hit the surface elsewhere and generate a cascade process; these grains form the “saltating” population. The second population consists of grains that are ejected with low energy, and stay close to the sand surface. These crawling grains form what is called the “reptating” population. Low-energy grains typically jump to a distance of a few hundred times the average grain size (Andreotti et al. 2002), and continue to roll on the sand surface after landing. The exchange flux between the reptating and the saltating populations is thought to be small (Anderson, 1987).

Here we adopt the view of ripple formation that was mathematically formalized by Anderson (1987, 1990). According to this interpretation, the only role of saltating grains is to bring energy into the system, extracting it from the wind that blows above the sand surface. In this view, ripple formation is entirely due to spatial changes in the reptation flux. Linear stability analysis of a model built on these premises shows that the wavelength of the fastest-growing perturbation is determined by the reptation length and not by the saltation length as previously suggested by Bagnold. The fastest-growing wavelength turns out to be roughly six times the mean reptation length.

However, there are two problems with Anderson’s model: The first is that large wavenumbers remain linearly unstable in his original model. Secondly, Anderson’s approach is purely linear and thus it is valid only for small ripples and short times.

We overcome the first problem by introducing a standard correction to the reptation flux, that makes it slightly smaller on the windward (stoss) slope and slightly larger on the lee slope. This correction to the reptation flux stabilizes short wavelengths and shifts the maximum of the reptation flux closer to the ripple crest, stopping excessive growth of the model ripples (Wilson, 1972). We then consider the full nonlinear version of the modified Anderson model and numerically solve the integro-differential equation that describes the dynamics of one-dimensional aeolian ripples. We also mention a weakly nonlinear expansion of the integro-differential model, along the lines previously discussed by Balmforth et al. (2001).

The rest of this paper is organized as follows: In section 2 we derive the model, in section 3 we discuss the results of linear stability analysis and in section 4 we discuss some numerical results. Finally, in section 5 we give a summary and some conclusions.

2. The integro-differential model

Following Anderson (1987) we build a heuristic model of sand transport based on the Exner equation,

$$(1 - \lambda_p) \rho_p \frac{\partial \zeta}{\partial t} = - \frac{\partial Q}{\partial x} , \quad (1)$$

where $\zeta(x, t)$ is the local height of the sand surface at point x and at time t , ρ_p is the density of a sand grain, λ_p is the porosity of the bed (typically taken as 0.35), and $Q(x, t)$ is the sand flux which includes both the saltation and the reptation fluxes. This equation shows that erosion ($\partial \zeta / \partial t < 0$) occurs in regions where the sediments flux is increasing ($\partial Q / \partial x > 0$), deposition ($\partial \zeta / \partial t > 0$) occurs where the flux is decreasing

($\partial Q / \partial x < 0$), and there is no change in the surface height where the transport rate is constant ($\partial Q / \partial x = 0$).

Saltating grains are accelerated by the wind to speeds that are close to the wind speed. These grains follow a ballistic path to the next impact site. If their arced trajectory is long compared to the size of the bed undulations, it seems plausible that the angle at which the grains descend back to the bed is dictated largely by the wind speed and that the flux of saltating grains is fairly uniform. Hence we assume that, for ripple dynamics, the flux of saltating grains, Q_s , can be taken as constant, and we do not consider it further in the Exner equation ($\partial Q_s / \partial x = 0$). However, we should keep in mind that saltating grains are the driving force of the reptation flux, and that for other aeolian bedforms, such as dunes, this approximation is not valid.

The reptation flux at a given point x and time t , Q_r , is obtained by a sum on all the grains that are passing by that point at that time. This is given by all the grains that have been ejected upwind and are still on their reptation flight. If all the grains had the same reptation length $\bar{\alpha}$, the flux at x would be proportional to the total number of grains that have been ejected between $x - \bar{\alpha}$ and x (note that this introduces a basic non-locality in the dynamics of aeolian ripples). In reality, the grains have a distribution of reptation lengths, and this should be taken into account in the expression for the flux. To derive an explicit expression for the reptation flux, we follow Anderson (1987) and write

$$Q_r^0(x) = m_p n_p \int_{-\infty}^{\infty} d\alpha p(\alpha) \int_{x-\alpha}^x N_{im}(x') dx', \quad (2)$$

where m_p is the mass of each particle, n_p is the average number of reptating grains ejected by the impact of one saltating grain, and $p(\alpha)$ is the probability distribution of reptation lengths. The value of n_p depends on the impact velocity and on the diameter of the grains (Forrest & Haff, 1992); in our model we assume n_p to be constant.¹ The probability distribution $p(\alpha)$ has to be determined experimentally; it is quantified by the “splash function” introduced by Ungar and Haff (1987).

Because the saltation flux is uniform, and the fixed angle ϕ at which the grains descend back to the ground is assumed to be constant, the number density of impacting grains changes only because of variations in the bed slope. Based on geometrical considerations, we obtain

$$N_{im}(x) = N_{im}^0 \left(1 + \frac{\tan \theta}{\tan \phi} \right) \cos \theta = N_{im}^0 \frac{1 + \zeta_x \cot \phi}{\sqrt{1 + \zeta_x^2}}, \quad (3)$$

where N_{im}^0 is the number density of impacting grains on a flat surface.

Expression (2) for the reptation flux leads to a situation where linear instability is not confined to a finite range of wavenumbers (Anderson, 1990). However, there are at

¹ Andreotti et al. (2002) argue that n_p should be smaller for a positive slope along the wind direction than for a negative slope.

least two physical effects that modify the expression of the reptation flux, and lead to a regularization of the system.

Following Prigozhin (1999), it can be shown that (assuming for simplicity that the bed slope is constant) the mean reptation length should be corrected as $\bar{a} = \bar{a}_0(1 - \cot \gamma \zeta_x)$, where \bar{a}_0 is the mean reptation length on a flat surface and γ is the ejection angle of reptating grains (see Figure 1). This correction leads to a mean reptation length that is shorter on the windward slope and longer on the leeward slope of the bedform.

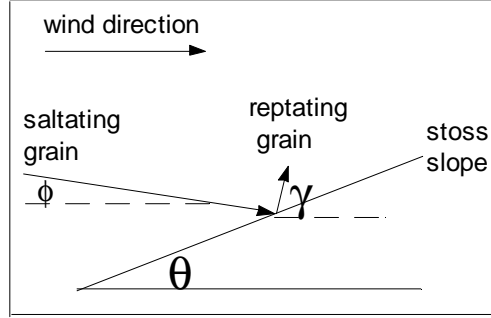


Fig.1: Schematic view of a typical collision. All angles are referred to the horizontal surface. A saltating grain approaches the inclined bed at angle ϕ . A reptating grain is ejected at an angle γ . The inclination of the bed is θ ($\theta > 0$ on the windward slope). The saltating grain ricochets (not shown in the figure) and continues the cascade.

A second effect is that part of the energy of the saltating grain is imparted to individual surface grains, which vibrate rapidly, and as a result can roll or slide down the slope (Hardisty & Whitehouse, 1988). Hardisty and Whitehouse termed this mechanism an “impact-induced gravity flow,” which acts to reduce the flux on the windward slope and to increase it on the lee face. Their empirical estimate of this correction gives:

$$Q_{slope} = Q_{flat} \left(\frac{\tan \theta_r}{\tan \theta_r + \tan \theta} \right) \approx Q_{flat} \left(1 - \frac{1}{\tan \theta_r} \tan \theta \right), \quad (4)$$

where Q_{flat} is the flux on a flat surface, Q_{slope} is the flux that includes the correction due to the gravity flow, θ_r is the angle of repose (usually taken to be 33°), and θ is the bed inclination (positive on the windward face).

Consideration of these two effects leads to the following expression for the reptation flux:

$$Q_r(x) = (1 - \mu \zeta_x) Q_r^0(x), \quad (5)$$

where the parameter μ heuristically includes both the Prigozhin and the Hardisty & Whitehouse corrections discussed above. The value of μ should be determined empirically.

Inserting expression (5) into the Exner equation (1) leads to the following equation

$$\zeta_t = Q_0 \left\{ \mu \zeta_{xx} \int_{-\infty}^{\infty} d\alpha p(\alpha) \int_{x-\alpha}^x F(x') dx' + (1 - \mu \zeta_x) \int_{-\infty}^{\infty} d\alpha p(\alpha) [F(x-\alpha) - F(x)] \right\}, \quad (6)$$

where $Q_0 = m_p n_p N_{im}^0 \cot \phi / (\rho_p (1 - \lambda_p))$ and $F(x) = (\tan \phi + \zeta_x) / \sqrt{1 + \zeta_x^2}$. Note that equation (6) breaks down when the lee slope of the ripples exceeds the impact angle ϕ of the saltating grains. In such conditions, the ratio N_{im} / N_{im}^0 becomes unphysically negative. Thus, we add the restriction $F(x) = 0$ if the bed slope exceeds the impact angle ϕ . This condition introduces a local shadowing effect and it is limited only to the lee slope, in contrast to a “complete shadowing” (Sharp, 1963) where the shadow zone can be extended to the windward slope.

3. Linear stability analysis

We assume an infinitesimal sinusoidal perturbation on an otherwise flat granular bed, given by

$$\zeta(x, t) = \zeta_0 \exp(ik(x - ct)), \quad (7)$$

where ζ_0 is the amplitude of the perturbation. Inserting (7) into (6), using the linear approximation $F(x) \approx \tan \phi + \zeta_x$ and discarding all nonlinear terms we obtain the dispersion relation (Anderson, 1987; Balmforth et al., 2001)

$$\frac{c}{Q_0} = 1 - \hat{p}(k) - ik\mu\bar{a} \tan \phi, \quad (8)$$

where $\hat{p}(k)$ is the Fourier transform of $p(\alpha)$, and $\bar{a} = \int_{-\infty}^{\infty} \alpha p(\alpha) d\alpha$ is the mean reptation length. If we choose for $p(\alpha)$ an exponential distribution

$$p(\alpha) = \begin{cases} \chi e^{-\chi\alpha} & \alpha > 0 \\ 0 & \alpha \leq 0 \end{cases}, \quad (9)$$

where χ is a parameter, we find that

$$\frac{c_r}{Q_0} = \frac{k^2}{k^2 + \chi^2}, \quad \frac{c_i}{Q_0} = \frac{k\chi}{k^2 + \chi^2} - \mu k \bar{a} \tan \phi, \quad (10)$$

where c_r is the real part of c , which determines the drift speed of the ripples, and c_i is the imaginary part that determines the growth rate of the perturbations. Instability occurs for $c_i \geq 0$. Figure 2 shows the dispersion curves for different values of μ , for $\phi = 10^\circ$ and for $\bar{a} = 1$ cm. The slope-dependent correction of the flux stabilizes the shorter wavelengths. Moreover, it is clear that the destabilizing effects must now overcome the stabilizing effect, introduced by including the flux correction, in order to form ripples. Note, also, that low impact angles favor destabilization of the bed. Careful experimental work is needed in order to measure the value of μ and give it a

plausible value. For example, for $\bar{a} = 1$ cm and $\phi = 10^0$, the maximum wavelength $\lambda_{\max} = 2\pi / k_{\max}$ increases from $4\bar{a}$ for $\mu = 0.1$ to $8\bar{a}$ for $\mu = 1.1$.

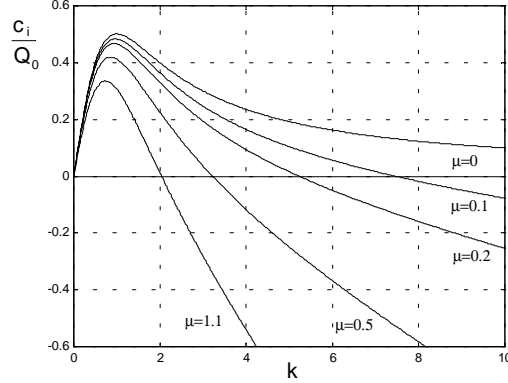


Fig. 2: Dispersion curves for the linearized version of model (6) for different values of μ and for the exponential probability distribution (9). Note that for $\mu = 0$, the original Anderson model is recovered. Higher values of μ result in a narrower range of unstable wavenumbers. Other parameter values are $\phi = 10^0$ and $\bar{a} = 1$ cm.

4. Numerical results

In this section we show some of the results obtained from numerically solving the integro-differential model (6) for realistic parameter values. The saltation flux is $N_{im}^0 = 10^7$ impacts $\text{m}^{-2} \text{s}^{-1}$, which according to Anderson (1990) is the saturated flux for a wind shear velocity of 0.5 m/s and for fine sand with grain diameter of 0.25 mm. For the probability distribution we choose $\chi = 1.651$, which gives $\bar{a} = 1$ cm. This value is close to the typical value of 8 mm reported for example by Andreotti et al. (2002). We solved eq. (6) numerically, assuming periodic boundary conditions and using an explicit finite-difference scheme on a spatial domain with size $L = 1$ m, grid spacing $\Delta x = 1$ mm and time step $\Delta t = 0.001$ seconds. Figure 3 shows the time evolution of the ripple pattern that emerges from random initial conditions. The initial evolution of the slightly perturbed bed surface is dictated by linear theory, and the wavelength of the fastest linearly growing wave dominates in the early stages of the evolution. Ripples begin as small amplitude bedforms or mottles on the surface (see fig. 2 in McEwan et al., 1992). The growing ripples remain almost symmetrical until the lee-slope angle exceeds the saltation impact angle. The asymmetry continues to develop as the ripples grow and the downwind slopes become steeper. Further development of the ripple pattern is due to a coarsening process, which leads to an increase of the ripple wavelength. Data from field observations (Werner & Gillespie, 1993) and from wind tunnel experiments (Anderson, 1990) are consistent with an asymptotic power-law increase of the mean ripple wavelength $\Lambda(t)$. Weakly nonlinear heuristic models of the dynamics of sand ripples (Csahók et al., 2000; Makse, 2000) predict a similar behavior, $\Lambda(t) \propto t^\beta$ with $0.27 < \beta < 0.5$. We find that the full model (6) also leads to approximate power-law growth of the average ripple wavelength, with $\beta \approx 0.35$, at intermediate times. At later times, the integro-differential model (6)

is consistent with a saturation of the ripple wavelength to a constant value (even though we cannot exclude a slow logarithmic growth of the wavelength).

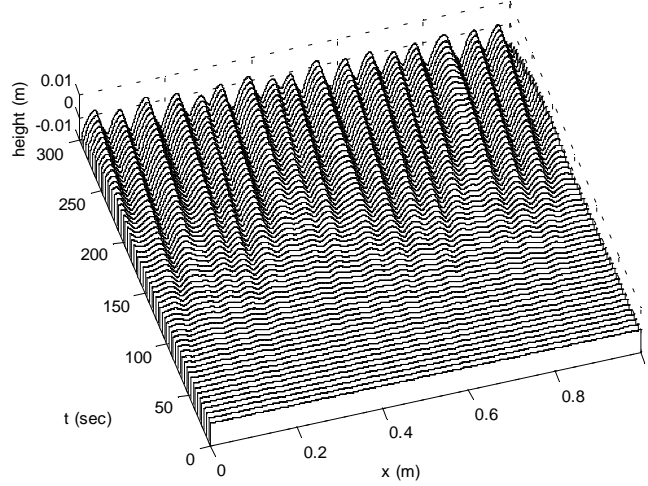


Fig. 3: Time evolution of the ripple pattern for $\mu = 0.9$ and uniform impact angle $\phi = 10^\circ$. Ripples grow from initial small random perturbations and their mean wavelength increases because of merging between different ripples. The asymmetry in the ripple profile starts to develop as the lee-slope angle exceeds the impact angle of saltating grains and a shadow zone appears. The drift velocity is approximately 1.2 cm/s, in good agreement with field measurements (Sharp, 1963).

5. Discussion and conclusions

In this work we have discussed an integro-differential model for the dynamics of aeolian sand ripples. The model is based on an extension of the classic approach by Anderson (1987). The present model relies upon the introduction of a physically-motivated flux correction, due to which the reptation flux decreases on the windward slope and increases on the lee slope. This type of correction is similar in shape to analogous terms introduced in the study of bedforms under water (e.g., Richards, 1980). Numerical solution of the integro-differential equation with realistic parameter values reveals the formation of ripples that are very close in size and shape to natural desert ripples. It remains for future experiments to determine the value of the phenomenological parameter μ , which defines the flux sensitivity to the bed slope.

In a previous work, a long-wave weakly nonlinear approximation of the integro-differential equation was introduced (Balmforth et al. 2001). In such a purely local approach, instability of the flat bed emerges due to the presence of a negative viscosity term, $-\zeta_{xx}$, which is stabilized at small wavelength by a hyperviscous term, $-\zeta_{xxxx}$. The growth of the ripple amplitude is saturated by the presence of quadratic and cubic nonlinear terms. A comparison between the results of the full integro-differential model and its weakly nonlinear expansion will be given in a future work, as well as an extension of the model to the case of two-dimensional ripples.

Finally, we note that in the present model we have assumed the saltation flux to be uniform, and the ripple wavelength depends solely on the reptation flux. Large enough undulations of the bed will break this ideal picture of a uniform saltation flux. In such cases, the saltation flux can depend on the bed topography, similarly to what has been discussed here for the reptation flux. Additionally, the feedback between the variations of the bed topography and the shear stress of the wind cannot be discarded for large bedforms (Richards, 1980). This may explain the formation of large-scale ripples, whose dominant wavelength may then depend on the mean saltation length as suggested by Ellwood et al. (1975).

References

- Anderson, R.S. (1987) A theoretical model for impact ripples. *Sedimentology*, **34**, 943-956.
- Anderson, R.S. (1990) Eolian ripples as example of self-organization in geomorphological systems. *Earth Sciences*, **29**, 77-96.
- Andreotti, B., Claudin, P., & Douady, S., (2002). *The European Physical Journal B*, in press
- Bagnold, R.A (1941) *The Physics of Blown Sand and Dunes*. Methuen, London, 265 pp.
- Balmforth, N.J., Provenzale, A., & Whitehead, J. (2001) The language of pattern and form. In *Geomorphological Fluid Mechanics*, N.J. Balmforth and A. Provenzale Eds., Springer.
- Cshaók, Z., Misbah, C., Rioual, F., & Valance, A. (2000) Dynamics of aeolian sand ripples. *The European Physical Journal E*, **3**, 71-86.
- Ellwood, J.M., Evans, P.D. & Wilson, I.G (1975) Small scale aeolian bedforms. *Journal of Sedimentary and Petrology*, **45**, 2, 554-561.
- Forrest, S.B., & Haff, P.K (1992) Mechanics of wind ripple stratigraphy. *Science*, **255**, 1240-1243.
- Hardisty, R.J.S. & Whitehouse, J. (1988) Evidence for a new sand transport process from experiments on Saharan dunes. *Nature*, **332**, 532-534.
- Hoyle, R.B., & Woods, A. (1997) Analytical model of propagating sand ripples. *Phys. Rev. E*, **56**, 6861.
- Makse, H.A (2000) Grain segregation mechanism in aeolian sand ripples. *The European Physical Journal E*, **1**, 127-135.
- McEwan, I.K., Willetts B.B., & Rice, A. (1992) The grain/bed collision in sand transport by wind. *Sedimentology*, **39**, 971-981.
- McLean, S. R (1990) The stability of ripples and dunes. *Earth-Science Reviews*, **29**, 131-144.
- Nishimori, H., & Ouchi, N. (1993) Formation of ripple patterns and dunes by wind-blown sand. *Phys. Rev. Lett.*, **71**, 197.
- Prigozhin, L. (1999) Nonlinear dynamics of aeolian sand ripples. *Physical Review E*, **60**, 729-733.
- Sharp, R.P (1963) Wind ripples. *J. Geology*, **71**, 617-636.
- Richards, K.J (1980) The formation of ripples and dunes on an erodible bed. *J Fluid Mech.* **99**, 597-618.
- Terzidis, O., Claudin, P., & Bouchaud, J.P (1998) A model for ripple instabilities in granular media. *The European Physical Journal B*, **5**, 245-249.
- Ungar, J., & Haff, P.K (1987) Steady state saltation in air. *Sedimentology*, **34**, 289-299.
- Valance, A., & Rioual, F. (1999) A nonlinear model for aeolian sand ripples. *The European Physical Journal B*, **10**, 543-548.
- Werner, B.T, & Gillespie, D.T (1993) Fundamentally discrete stochastic model for wind ripples. *Physical Review letters*, **71**, 19, 3230-3233.
- Wilson, I.G, (1972) Aeolian bedforms-their development and origins. *Sdimentology*, **19**, 173-210.